PERGAMON

International Journal of Solids and Structures 36 (1999) 269–284

INTERNATIONAL JOURNAL OF
SOLIDS and
STRUCTURES

Nonlinear diffusion-induced stresses in a long bar of square cross section

Chi-Chuan Hwang[a,]*, Senpuu Lin, Hsin-Sen Chu[b], Woei-Shyan Lee[c]

[a]*Department of Mechanical Engineering, Chung Yuan University, Chung Li, Taiwan 32023, Republic of China*
[b]*Department of Mechanical Engineering, National Chiao Tung University, Hsinchu,*
Taiwan 30050, Republic of China
[c]*Department of Mechanical Engineering, National Cheng-Kung University, Tainan,*
Taiwan 70101, Republic of China

Received 27 March 1997; in revised form 17 October 1997

Abstract

This paper is to investigate the nonlinear effect of the self-induced electric field on the diffusion-induced stresses in a long bar. We first approximate the nonlinear concentration-dependent diffusivity as a series of third-degree polynomials by the least-squares curve-fitting techniques, and then calculate the distributions of concentration by the Galerkin method. Afterwards, the diffusion-induced stresses inside the bar are determined analytically by introducing the Goodier displacement potential and Airy stress function. It is found that the nonlinear self-induced electric fields can depress both the concentration gradient and the maximum diffusion-induced stresses apparently, and these effects are more significant at short times than at long times. © 1998 Elsevier Science Ltd. All rights reserved.

1. Introduction

Diffusion-induced stresses, during mass transfer, can change the mechanical properties in metal systems such as hardening (Reed-Hill, 1973; Hertzberg, 1983). The diffusion-induced stresses in semiconductor materials during diffusion processes have been studied extensively over recent decades, because they can cause dislocation generation which affects solute distribution and subsequent electronic properties (Bardsley, 1960). The diffusion-induced stresses are built up by composition inhomogeneity during mass transfer, i.e., they are caused by concentration gradients, similar to those caused by temperature gradients in an otherwise unstressed body. Prussin (1961) was the first to analyze the transverse stresses developed in a thin plate during diffusion process. The diffusion-induced stresses related to the dislocation density was studied in detail by Tuck

---

* Corresponding author.

PII: S0020–7683(97)00324–7

(1974). Li (1978) solved the diffusion-induced stresses in a single-phase elastic medium of various geometries and corrected an error made by Prussin (1961). Further, Lee and Li (1981) proposed that the most rapid diffusion processes occur without generation of dislocation. Lee and Ouyang (1987) derived a general solution for boundary stress as a function of time. Chu and Lee (1990) obtained diffusion-induced stresses in two-phase elastic media. Chu and Lee (1993) carried out a study of diffusion-induced stresses in a long bar of square cross section. Hwang et al. (1994) further investigated diffusion-induced stresses in a long bar under an electric field. However, the above calculations of diffusion-induced stresses only treated the simple linear systems with a constant diffusivity. Because the chemical stresses arising from diffusion are not only related to geometric shape but also related to the boundary conditions, Larché and Cahn (1982, 1985) studied the stress dependence of the local diffusion flux in crystalline solids. Chu and Lee (1994) investigated the effect of chemical stresses on diffusion. In order to accurately predict the electrical properties of the device, an accurate description of the final concentration distributions is necessary. In 1963, Weisberg and Blanc (1963) studied the nonlinear interstitial-substitutional equilibrium Zinc diffusion in GaAs. Hu and Schmidt (1968) introduced a concentration dependent diffusion model which included the effects of both the charged vacancy reaction and the impurity-induced electric fields. Warner and Wilson (1980) investigated the effect of the self-induced electric field on diffusion by numerical method. Kath and Cohen (1982) studied the waiting-time behavior in a nonlinear diffusion equation using singular-perturbation techniques. King (1988) obtained the approximate similarity solutions to a nonlinear diffusion equation in one and two dimensions. Schwendeman (1990) calculated the fully two-dimension nonlinear diffusion of impurities in semiconductors by numerical techniques. Moreover, Menon et al. (1993) studied the nonlinear diffusion in Cu–Au multilayer thin films.

Lin and Hwang (1995) investigated the nonlinear effect of self-induced electric field on diffusion-induced stresses in a thin plate. However, in practice, the application of mass transfer to manufacture is not confined to the generalized one-dimensional diffusion processes. It prompted us to investigate the nonlinear diffusion-induced stresses in a long bar of square cross section. In this work, we first approximate the nonlinear concentration-dependent diffusivity as a series of third-degree polynomials by the least-squares curve-fitting techniques, and then calculate the distributions of concentration by the Galerkin method. With these results, the diffusion-induced stresses inside the bar are determined analytically by introducing the Goodier displacement potential and Airy stress function. A comparison is made between the present results and the linear diffusivity model to investigate the nonlinear effect of self-induced electric field on the diffusion-induced stresses in a long bar.

2. Analysis of concentration distribution

Consider a long bar of isotropic material with square cross section in the region $-a \leqslant X, Y \leqslant a$, as shown in Fig. 1. Initially there is no charged impurity inside the bar, while as process begins, the concentration at the outer surface is maintained constant at C_s during diffusion. The diffusion with the nonlinear effect of the self-induced electric field can be modeled as in Warner and Wilson (1980). Hence, the concentration $C(X, Y, t)$ for arsenic in silicon is described by the following equation:

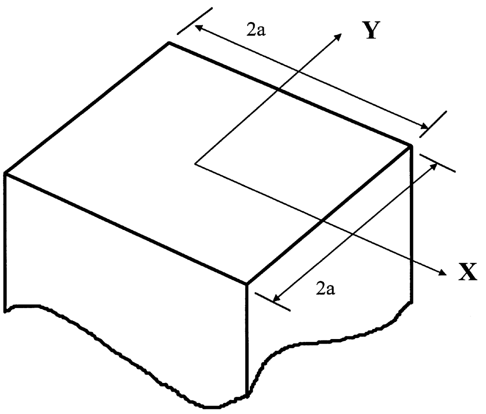

Fig. 1. Physical configuration of a long bar.

$$\frac{\partial \alpha}{\partial t} = \frac{\partial}{\partial X}\left[D(\alpha)\frac{\partial \alpha}{\partial X}\right] + \frac{\partial}{\partial Y}\left[D(\alpha)\frac{\partial \alpha}{\partial Y}\right] \tag{1}$$

where

$$\alpha = \frac{C}{2n_i}$$

and $D(\alpha)$, the concentration dependent diffusion coefficient, is defined by

$$D(\alpha) = D_0\frac{1+\beta[\alpha+\sqrt{\alpha^2+1}]}{1+\beta}\left[1+\frac{\alpha}{\sqrt{\alpha^2+1}}\right] \tag{2}$$

here n_i is the intrinsic carrier concentration, D_0 is the phenomenological low concentration diffusion constant and $\beta = 100$ for arsenic (Warner and Wilson, 1980).

The corresponding initial and boundary conditions just mentioned are

$$\begin{aligned} &\alpha(X, Y, 0) = 0, \\ &\alpha(\pm a, Y, t) = \alpha_s, \\ &\alpha(X, \pm a, t) = \alpha_s \end{aligned} \tag{3}$$

where

$$\alpha_s = \frac{C_s}{2n_i}.$$

Then, if the dimensionless variables

$$x = \frac{X}{a}, \quad y = \frac{Y}{a}, \quad \tau = \frac{D_0 t}{a^2}, \quad 1+\alpha^* = \frac{\alpha}{\alpha_s} = \frac{C}{C_s} \tag{4}$$

are introduced, eqns (1)–(3) will take the forms:

$$\frac{\partial \alpha^*}{\partial t} = \frac{\partial}{\partial x}\left[D(\alpha^*)\frac{\partial \alpha^*}{\partial x}\right] + \frac{\partial}{\partial y}\left[D(\alpha^*)\frac{\partial \alpha^*}{\partial y}\right], \tag{5}$$

$$D(\alpha^*) = \frac{1+\beta[\alpha_s(1+\alpha^*)+\sqrt{\alpha_s^2(1+\alpha^*)^2+1}]}{1+\beta}\left[1+\frac{\alpha_s(1+\alpha^*)}{\sqrt{\alpha_s^2(1+\alpha^*)^2+1}}\right] \tag{6}$$

and

$$\begin{aligned} \alpha^*(x,y,0) &= -1, \\ \alpha^*(\pm 1, y, \tau) &= 0, \\ \alpha^*(x, \pm 1, \tau) &= 0. \end{aligned} \tag{7}$$

To be suitable for solving the nonlinear equation by the Galerkin method, eqn (6), which referred to the diffusion coefficient, may be approximated in a series of third-degree polynomials by the least-squares curve-fitting method as the following form:

$$D(\alpha^*) = B_0 + B_1\alpha_s(1+\alpha^*) + B_2\alpha_s^2(1+\alpha^*)^2 + B_3\alpha_s^3(1+\alpha^*)^3, \tag{8}$$

the coefficients can be regarded as phenomenological parameters.

Solving the above equations through the Galerkin method, we selected the solution

$$\alpha^*(x,y,\tau) = \sum_{j=0}^{\infty}\sum_{i=0}^{\infty} A_{ij}(\tau)\cos(\rho_j x)\cos(\omega_i y) \tag{9}$$

where

$$\rho_j = \frac{2j+1}{2}\pi, \omega_i = \frac{2i+1}{2}\pi, \tag{10}$$

and $\cos(\rho_j x)\cos(\omega_i y)$ satisfied the boundary conditions, then $A_{ij}(\tau)$ for $i, j = 0, 1, 2, \ldots, \infty$ can be determined from the set of the coupled nonlinear equations in Appendix A with the initial condition of $A_{ij}(0) = -4(-1)^{i+j}/(\rho_j\omega_i)$.

The infinite series in eqn (9) is truncated at $j = J$, $i = I$ so as to obtain the results to four significant digits. For accuracy, in the present calculations, a choice of $I = J = 30$ is made and $A_{ij}(\tau)$ less than 10^{-8} is deleted. Hence, the solution of the concentration can be expressed by

$$\frac{C}{C_{\mathrm{s}}} = 1+\sum_{j=0}^{J}\sum_{i=0}^{I} A_{ij}(\tau)\cos(\rho_j x)\cos(\omega_i y). \tag{11}$$

3. Diffusion-induced stresses

As the concentration distribution is obtained one can proceed to find the diffusion-induced stress distributions. The derivation of stress distribution arising from solute transfer is similar to that arising from heat transfer, if the thermal expansion coefficient and temperature are replaced by one-third of partial molal volume and concentration, respectively (Chu and Lee, 1993; Li, 1978).

In the present work, from the practical point of view, we assume that it is a quasistatic and uncoupled diffusion-induced-stress problem. Further, because of the long bar, we consider only the elastic plane strain states. In a similar way to Nowinski's work (1978), we introduce the dimensionless Goodier displacement potential ϕ_0 and the Airy stress function ϕ_{A} which, respectively, have to satisfy

$$\Delta\phi_0 = C/C_{\mathrm{s}} \tag{12}$$

$$\Delta\Delta\phi_{\mathrm{A}} = 0 \tag{13}$$

where $\Delta = \partial^2/\partial x^2+\partial^2/\partial y^2$ and C/C_{s} is shown by eqn (11). Then, in similar procedures to the work of Iwaki and Kobayashi (1981), the diffusion-induced stresses are given by

$$\sigma_{ij} = \sigma_{0ij}+\sigma_{A_{ij}}, \tag{14}$$

where

$$\begin{aligned}
\sigma_{0xx} &= -\frac{\partial^2\phi_0}{\partial y^2},\\
\sigma_{0yy} &= -\frac{\partial^2\phi_0}{\partial x^2},\\
\sigma_{0zz} &= -\Delta\phi_0,\\
\sigma_{0xy} &= \frac{\partial^2\phi_0}{\partial x\,\partial y},
\end{aligned} \tag{15}$$

and

$$\sigma_{Axx} = \frac{1}{2\mu}\frac{\partial^2\phi_{\mathrm{A}}}{\partial y^2},$$

$$\sigma_{Ayy} = \frac{1}{2\mu}\frac{\partial^2\phi_{\mathrm{A}}}{\partial x^2},$$

$$\sigma_{Azz} = \frac{v}{2\mu}\Delta\phi_{\mathrm{A}},$$

$$\sigma_{Axy} = -\frac{1}{2\mu}\frac{\partial^2\phi_{\mathrm{A}}}{\partial x\,\partial y}. \tag{16}$$

Here μ is the Lamé constant and v is the Poisson's ratio. It should be noted that the dimensionless forms of ϕ_0, ϕ_{A}, and σ_{ij} are given by

$$\phi_0 = \frac{\Phi_0}{a^2\Lambda}, \quad \phi_{\mathrm{A}} = \frac{\Phi_{\mathrm{A}}}{a^2\Lambda}, \quad \sigma_{ij} = \frac{\Sigma_{ij}}{2\mu\Lambda}, \tag{17}$$

where Φ_0, Φ_{A}, Σ_{ij} are the dimensional Goodier displacement potential, the Airy stress function and stresses, respectively, and $\Lambda = (1+v)\bar{V}C_{\mathrm{s}}/3(1-v)$. Here $\bar{V}$ is the partial molal volume of solute and assumed to be constant (Li, 1978). The traction-free boundary conditions are adopted, i.e.,

$$\sigma_{xy}(x, \pm 1, \tau) = \sigma_{yy}(x, \pm 1, \tau) = 0, \tag{18a}$$

$$\sigma_{xx}(\pm 1, y, \tau) = \sigma_{xy}(\pm 1, y, \tau) = 0. \tag{18b}$$

Since the dimensionless concentration C/C_{s} has been found in the preceding section, by substituting eqn (11) into eqn (12), we have a particular solution:

$$\phi_0 = \sum_{j=0}^{J}\sum_{i=0}^{I} -\frac{1}{\rho_j^2+w_i^2}A_{ij}(\tau)\cos(\rho_j x)\cos(\omega_i y) + \frac{1}{4}(x^2+y^2). \tag{19}$$

The Airy stress function is constructed in the form

$$\phi_{\mathrm{A}} = \phi_1 + \phi_2, \tag{20}$$

thus

$$\sigma_{A_{ij}} = \sigma_{1ij} + \sigma_{2ij}, \tag{21}$$

where the stresses σ_{1ij} and σ_{2ij} are derived from ϕ_1 and ϕ_2, respectively.

An admissible solution of the function ϕ_1, suitable for the present problem, has the form (Nowinski, 1978)

$$\phi_1 = 2\mu\left\{\sum_{j=0}^{J}[E_j\cosh(\rho_j y) + F_j\sinh(\rho_j y) + G_j y\cosh(\rho_j y) + H_j y\sinh(\rho_j y)]\cos(\rho_j x) + \frac{1}{4}(x^2+y^2)\right\}, \tag{22}$$

where the unknowns E_j, F_j, G_j and H_j are determined so as to satisfy the boundary conditions of eqn (18a) at the edges along $x = \pm 1$

$$\sigma_{0yy}(x, \pm 1, \tau) + \sigma_{1yy}(x, \pm 1, \tau) = 0,$$
$$\sigma_{0xy}(x, \pm 1, \tau) + \sigma_{1xy}(x, \pm 1, \tau) = 0. \tag{23}$$

Consequently, one has

$$\begin{aligned} E_j &= \left\{ -\sinh \rho_j \sum_{i=0}^{I} \frac{(-1)^i \omega_i}{\rho_j^2 + \omega_i^2} A_{ij}(\tau) \right\} / \Delta_j, \\ F_j &= 0, \\ G_j &= 0, \\ H_j &= \left\{ \cosh \rho_j \sum_{i=0}^{I} \frac{(-1)^i \omega_i}{\rho_j^2 + \omega_i^2} A_{ij}(\tau) \right\} / \Delta_j, \end{aligned} \tag{24}$$

where

$$\Delta_j = \rho_j + \frac{\sinh(2\rho_j)}{2}. \tag{25}$$

To satisfy the boundary conditions of eqn (18b) at the edges along $y = \pm 1$, the function ϕ_2 is taken in the form (Nowinski, 1978)

$$\phi_2 = 2\mu \cos(\gamma x)[P \cosh(\gamma y) + Q\gamma y \sinh(\gamma y)], \tag{26}$$

which automatically satisfies eqn (13).

In determining ϕ_2, the subsequent boundary conditions from the above calculation require

$$\sigma_{2yy}(x, \pm 1, \tau) = \sigma_{2xy}(x, \pm 1, \tau) = 0, \tag{27}$$

and

$$\sigma_{2xx}(\pm 1, y, \tau) = -\sigma_{0xx}(\pm 1, y, \tau) - \sigma_{1xx}(\pm 1, y, \tau),$$
$$\sigma_{2xy}(\pm 1, y, \tau) = -\sigma_{0xy}(\pm 1, y, \tau) - \sigma_{1xy}(\pm 1, y, \tau). \tag{28}$$

By condition (27), one finds that γ must be the root of the transcendental relation

$$\sinh(2\gamma) + (2\gamma) = 0, \tag{29}$$

with

$$P = -\frac{\gamma \sinh \gamma}{\cosh \gamma} Q. \tag{30}$$

Equation (29) has infinitely many complex roots. Let γ_n by the nth root, thus ϕ_2 now can be expressed as the following series

$$\phi_2 = 2\mu \sum_{n=1}^{N} K_n f_n(x, y), \tag{31}$$

where

$$f_n(x, y) = \cos(\gamma_n x)[-\sinh \gamma_n \cosh(\gamma_n y) + y \cosh \gamma_n \sinh(\gamma_n y)], \tag{32}$$

and K_n's are unknown complex coefficients. The remaining work of solving ϕ_2 is to determine K_n's by using eqn (28). By using eqn (31), with eqn (32), for the left-hand side of (28) and by using the known functions ϕ_0 and ϕ_1 for the right-hand side of (28), the exact solution is expected. However, due to the constraint of the form of power series, these coefficients can only be approximately determined by numerical methods. In this work, they are determined by the method of least squares, so the boundary conditions, (28), may be satisfied at a number of midpoints (y_m, $m = 1, 2, \ldots, M$) across the surfaces at $x = \pm 1$. Thus, we can establish the simultaneous equations

$$[S]_{2M \times 2N}[U]_{2N \times 1} = [V]_{2M \times 1}, \tag{33}$$

where the elements of each matrix in eqn (33) are shown in Appendix B. After ϕ_0, ϕ_1 and ϕ_2 have been solved, we then can combine eqns (14)–(16) and eqns (20)–(21) to obtain the dimensionless diffusion-induced stress σ_{ij}.

4. Results and discussion

The diffusivity is approximately constant at low concentration levels (Warner and Wilson, 1980; King, 1988; Schwendeman, 1990). While, for arsenic diffusion in silicon, and as an example of high concentration levels, Warner and Wilson (1980) take $\alpha_s = 20$ (this corresponds to a surface concentration at forty times the intrinsic carrier concentration), the diffusivity is concentration-dependent, and the nonlinear effect on concentration is increased with increasing α_s. From our previous work (Lin and Hwang, 1995), the concentration-dependent coefficients B_0–B_3 of eqn (8) are calculated by the least-squares curve-fitting method. As we known, a higher-degree polynomials will reduce the deviations of the points from a curve, and one increases the degree of approximating polynomial as long as there is a statistically significant decrease in the variance. The criterion of choosing the optimum degree with good precision is that the sum of the deviations squared of the points from the curve should continually decrease as the degree of the polynomial is raised (Gerald and Wheatley, 1994). For simplicity, in the present study, the nonlinear case of $\alpha_s = 10$ is considered. Then, $B_0 = 5.44321 \times 10^{-1}$, $B_1 = 3.62028$, $B_2 = 6.32417 \times 10^{-2}$, $B_3 = -3.53349 \times 10^{-3}$, and the variance is 4.89226×10^{-3}. As shown in Fig. 2 of our previous study (Lin and Hwang, 1995), the least-squares approximation is one of good fits to eqn (6).

To investigate the nonlinear effect of the self-induced electric field, comparing these results of nonlinear D model with the solution to a linear case with a constant effective diffusivity of $D(\alpha^*) = 1$ (linear D_0 model). The contours of concentration C/C_s at $\tau = 0.01$ in both nonlinear and linear models are plotted in Fig. 2. Because the contours are symmetric, we only show them in the one-eighths domain of $0 \leqslant x \leqslant 1$, $0 \leqslant y \leqslant 1$. It is easy to see that the concentration gradient in the nonlinear diffusivity model is smaller than that in the linear one. The distribution of C/C_s

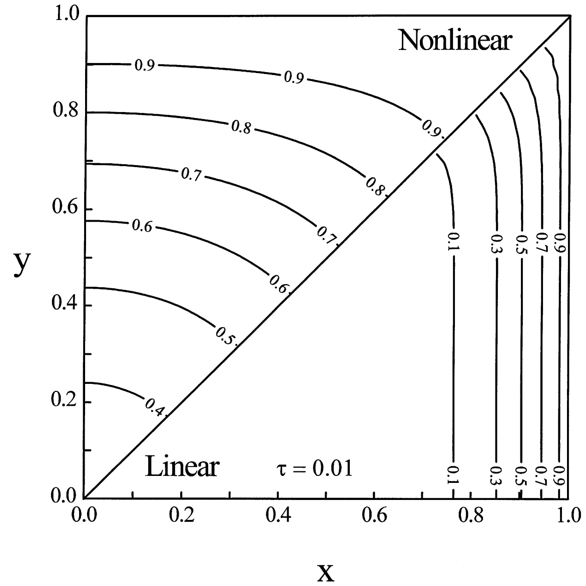

Fig. 2. ConcentrationC/C_s contours at $\tau = 0.01$.

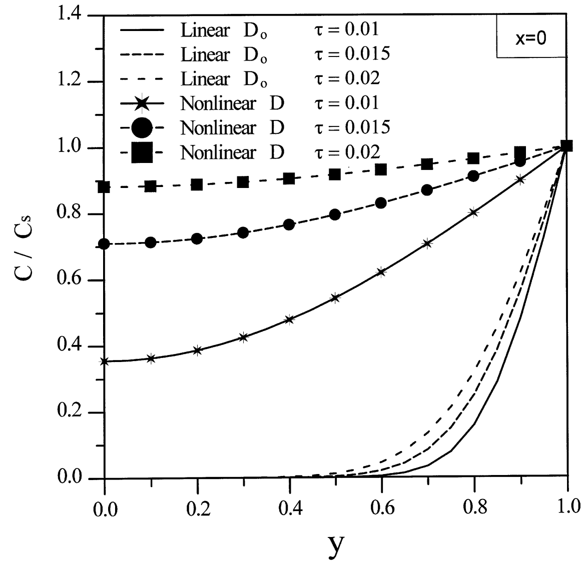

Fig. 3. Concentration C/C_s distribution along y axis.

along the y axis at different times is shown in Fig. 3. It is found that the nonlinear self-induced electric fields can depress the concentration apparently in a short time. Further, as the time is increased, the concentration gradient is decreased in both models. These results are in conformity

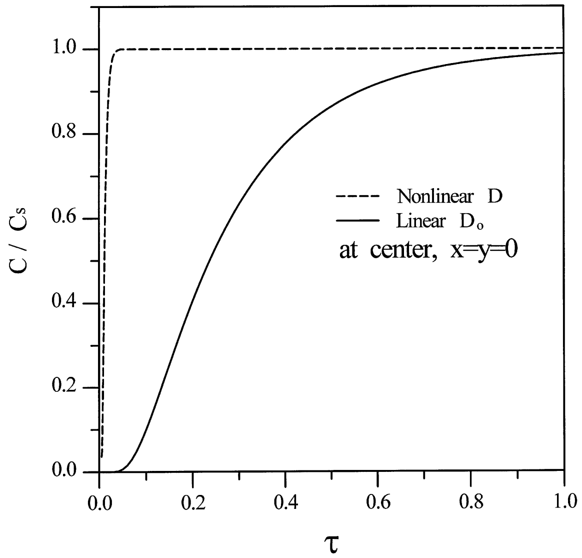

Fig. 4. The evolution of concentration C/C_s at $x = 0$, $y = 0$.

with the Warner and Wilson (1980) work. Also, in Fig. 4, the evolution of C/C_s at $x = 0$, $y = 0$ is plotted. We find that the difference between the nonlinear model and the linear one is increased with increasing time extremely at short times ($\tau < 0.025$). But, as the time is increased long enough (for example, $\tau = 0.5$), i.e. at a long time diffusion, because the concentration distribution will approach uniform, the nonlinear effects at long times will be less apparent than at short times.

In this article, the stress that is calculated is the equivalent shear stress Σ_e which is defined by

$$\Sigma_e = \sqrt{S_{ij}S_{ij}/2}, \tag{34}$$

where S_{ij} is the stress deviator $S_{ij} = \Sigma_{ij} - \Sigma_{kk}\delta_{ij}/3$. We choose Σ_e to be calculated because it is a measure of that part of the stress tensor which causes plastic deformation by dislocation slip. Although, in the diffusion-induced stress analysis, we have obtained the analytical solutions of the stress tensor, only numerical results are in fact calculated (Hwang et al., 1993). If the local equivalent shear stress Σ_e exceeds the critical value, i.e. the yield stress, a dislocation occurs in the bar. Their presence may degrade both the mechanical and electronic properties of the material.

In the present calculations of the diffusion induced-stresses, a choice of $N = 19$ and $M = 21$ is made in order to provide better accuracy (Iwaki and Kobayashi, 1981, 1986) and the Poisson ratio is chosen as $v = 0.3$. The contours of non-dimensional $\sigma_e = 100(\Sigma_e/2\mu\Lambda)$ at different times in both models are plotted in Fig. 5. As might be expected, the differences between the nonlinear model and the linear one are seen clearly. It is found that the maximum equivalent shear stress developed in the bar is located at the midedge in the beginning of diffusion. Further, the maximum σ_e is decreases with increasing time for both models. In Fig. 6, we show the distribution of σ_e along the y axis at different times. It is found that the σ_e distribution can be depressed by the nonlinear effect of the self-induced electric fields. In addition, for instance at the time of $\tau = 0.01$, we also find

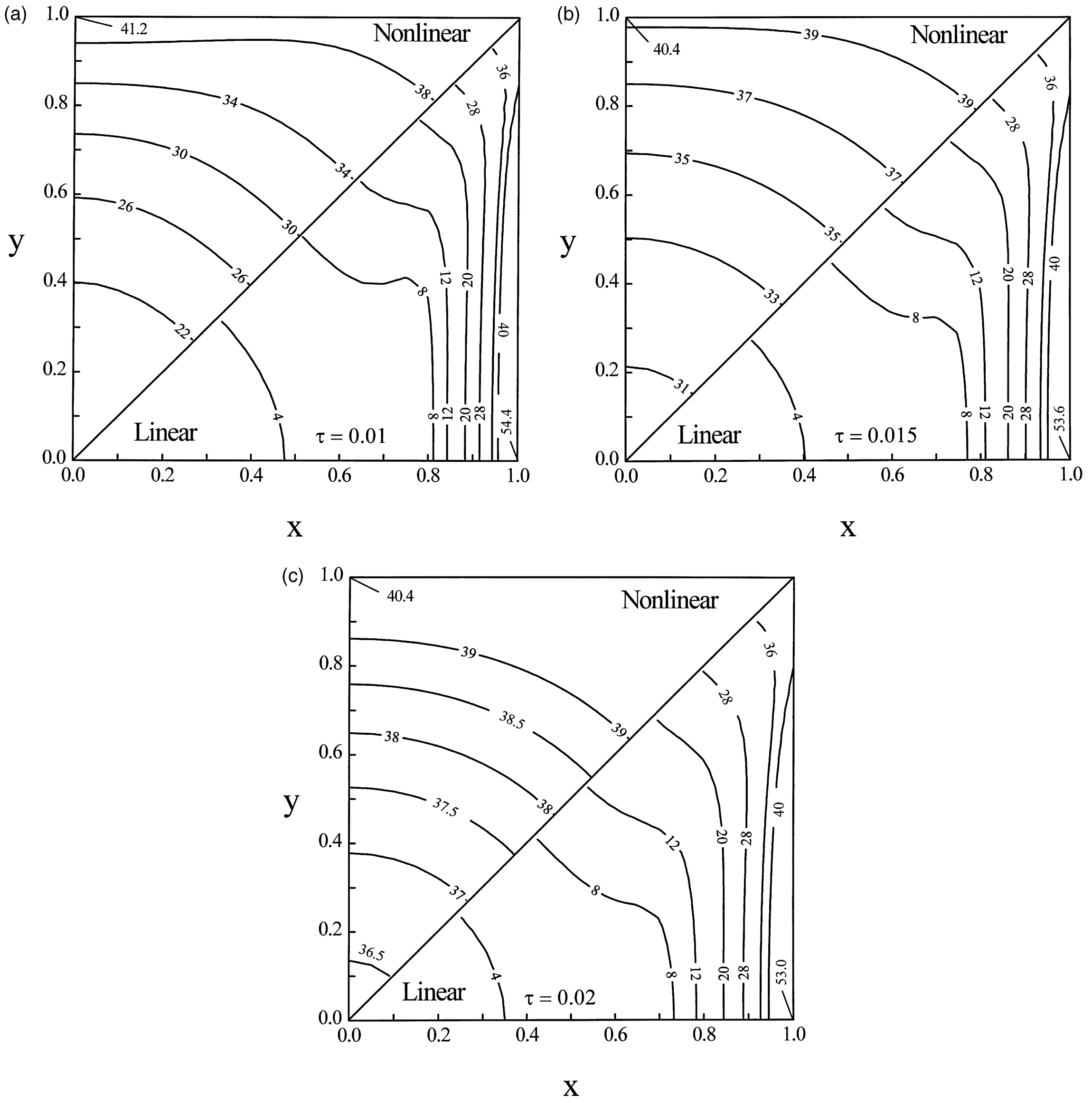

Fig. 5. Non-dimensional equivalent shear stress $\sigma_e = 100(\Sigma_e/2\mu\Lambda)$ contours (a): $\tau = 0.01$, (b): 0.015, (c): 0.02.

from Fig. 5(a), the maximum equivalent shear stress of the nonlinear model may be less than 20% that of the linear one.

Finally, in Fig. 7, the evolutions of the maximum σ_e developed at the midedge ($x = 0, y = 1$) of the bar for both models are demonstrated. With increasing time, the maximum σ_e in both models will approach $100|\sigma_{zz}|/\sqrt{3}$ which is the value of σ_e when $\sigma_{xx} = 0 = \sigma_{yy} = \sigma_{xy}$, i.e. the concentration distribution is approximately uniform in the x–y plane of the bar. So, the dimensionless value of $100|\sigma_{zz}|/\sqrt{3}$ is equal to $100(1-\nu)/\sqrt{3}$ which is the same as the value in a thin slab. We also find

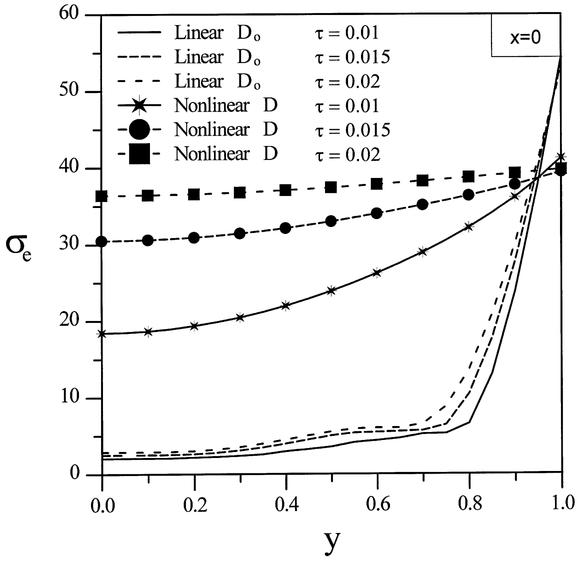

Fig. 6. Non-dimensional equivalent shear stress $\sigma_e = 100(\Sigma_e/2\mu\Lambda)$ distribution along y axis.

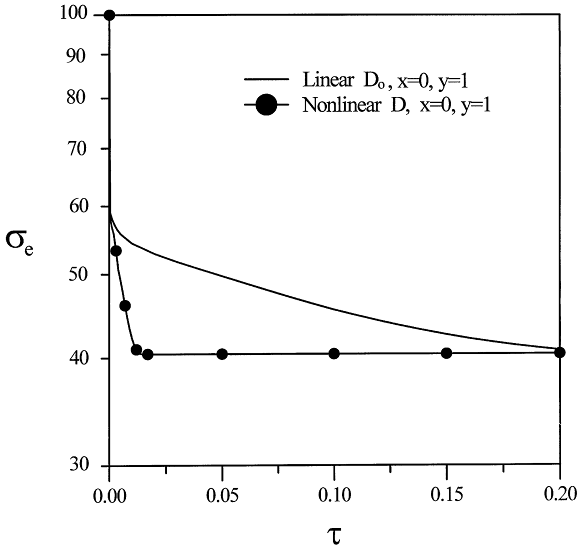

Fig. 7. The evolution of non-dimensional equivalent shear stress $\sigma_e = 100(\Sigma_e/2\mu\Lambda)$ developed at the midedge of the bar.

that the difference of σ_e between the nonlinear model and the linear one is increased with increasing time at short times, but is decreased with increasing time at long times. As the time is increased long enough, there will be significant difference in σ_e between the nonlinear model and the linear one. This means that the nonlinear effects on the induced-stress σ_e are more apparent at short times than at long times.

For an example of boron diffusion in silicon, the elastic constant of silicon at 1225°C for diffusion into a $\{100\}$ surface, $2\mu(1+v)/(1-v)$, is a value of 2.156×10^{12} dynes/cm^2 (215.6 GPa). And, the values of $\bar{V}$ and C_s for boron at 1225°C are, respectively, 5.6×10^{-24} cm^3/atoms and 5×10^{20} atoms/cm^3 (Prussin, 1961). Then, a value of $2\mu\Lambda$ in eqn (17) is calculated to be 2.01×10^9 dynes/cm^2 (201 MPa), which is the maximum Σ_e in both models at the beginning of diffusion. Further, if we assumed the value of β in eqn (2) is also equal to 100 in this case, the maximum Σ_e in both nonlinear and linear models are, respectively, 0.83×10^9 dynes/cm^2 (83 MPa) ($\sigma_e = 41.2$) and 1.1×10^9 dynes/cm^3 (110 MPa) ($\sigma_e = 54.4$) at $\tau = 0.01$. The yield stress in silicon whiskers is given by 5.5×10^9 dynes/cm^2 (550 MPa) at 800°C, and extrapolating the data to 1225°C reduced the value of the yield stress by an order of magnitude. With a comparison between the maximum Σ_e and the yield stress, it is found that the diffusion-induced stresses may not be ignored in semiconductor materials during diffusion processes especially at short times.

5. Conclusions

In this paper, we have investigated the nonlinear effect of the self-induced electric field on the diffusion-induced stresses in a long bar of square cross section. The mass transfer process of constant surface concentration is considered. We first approximate the nonlinear concentration-dependent diffusivity as a series of third-degree polynomials by the least-squares curve-fitting techniques, and then calculate the distributions of concentration by the Galerkin method. Afterwards with these results, the diffusion-induced stresses inside the bar are determined analytically by introducing the Goodier displacement potential and Airy stress function. It is found that the maximum equivalent shear stress developed in the bar is located at the midedge in the beginning of diffusion. With increasing time, both the concentration gradient and the maximum induced-stresses are decreased. Further, the nonlinear self-induced electric fields can depress the concentration gradient and the maximum diffusion-induced stresses, and these effects are more apparent at short times than at long times.

Acknowledgements

The authors acknowledge with appreciation the financial support (Grant No. NSC 84-2212-E-033-002) provided by the National Science Council of the Republic of China.

Appendix A

$$\frac{\mathrm{d}A_{ij}}{\mathrm{d}\tau} = -\bar{B}(\rho_j^2+\omega_i^2)A_{ij}-\bar{C}\sum_{l=0}^{j}\sum_{k=0}^{i}A_{i-k,j-l}A_{kl}[(\rho_l^2+\omega_k^2)\bar{F}-\rho_{j-l}\rho_l\bar{G}-\omega_{i-k}\omega_k\bar{H}]$$

$$-\bar{D}\sum_{l=0}^{j}\sum_{k=0}^{i}\sum_{q=0}^{l}\sum_{p=0}^{k}A_{i-k,j-l}A_{k-p,l-q}A_{pq}[(\rho_q^2+\omega_p^2)\bar{I}-2\rho_{l-q}\rho_q\bar{J}-2\omega_{k-p}\omega_p\bar{K}]$$

$$
-\bar{E}\sum_{l=0}^{j}\sum_{k=0}^{i}\sum_{q=0}^{l}\sum_{p=0}^{k}\sum_{s=0}^{q}\sum_{r=0}^{p} A_{i-k,j-l}A_{k-p,l-q}A_{p-r,q-s}A_{rs}
$$
$$
\times[(\rho_s^2+\omega_r^2)\bar{L}-3\rho_{q-s}\rho_s\bar{M}-3\omega_{p-r}\omega_r\bar{N}] \quad \text{for} \quad i,j=0,1,2,\ldots,\infty
$$

where

$$
\begin{aligned}
\bar{B} &= B_0+B_1\alpha_s^2 + B_3\alpha_s^2+B_3\alpha_s^3,\\
\bar{C} &= B_1\alpha_s+2B_2\alpha_s^2+3B_3\alpha_s^3,\\
\bar{D} &= B_2\alpha_s^2+3B_3\alpha_s^3,\\
\bar{E} &= B_3\alpha_s^3,
\end{aligned}
$$

$$
\begin{aligned}
\bar{F} &= \int_{-1}^{1}\int_{-1}^{1}\cos(\rho_j x)\cos(\rho_{j-l}x)\cos(\rho_l x)\cos(\omega_i y)\cos(\omega_{i-k}y)\cos(\omega_k y)\,\mathrm{d}x\,\mathrm{d}y,\\
\bar{G} &= \int_{-1}^{1}\int_{-1}^{1}\cos(\rho_j x)\cos(\rho_{j-l}x)\sin(\rho_l x)\cos(\omega_i y)\cos(\omega_{i-k}y)\cos(\omega_k y)\,\mathrm{d}x\,\mathrm{d}y,\\
\bar{H} &= \int_{-1}^{1}\int_{-1}^{1}\cos(\rho_j x)\cos(\rho_{j-l}x)\cos(\rho_l x)\cos(\omega_i y)\sin(\omega_{i-k}y)\sin(\omega_k y)\,\mathrm{d}x\,\mathrm{d}y,
\end{aligned}
$$

$$
\begin{aligned}
\bar{I} &= \int_{-1}^{1}\int_{-1}^{1}\cos(\rho_j x)\cos(\rho_{j-l}x)\cos(\rho_{l-q}x)\cos(\rho_q x)\\
&\quad\times\cos(\omega_i y)\cos(\omega_{i-k}y)\cos(\omega_{k-p}y)\cos(\omega_p y)\,\mathrm{d}x\,\mathrm{d}y,\\
\bar{J} &= \int_{-1}^{1}\int_{-1}^{1}\cos(\rho_j x)\cos(\rho_{j-l}x)\sin(\rho_{l-q}x)\sin(\rho_q x)\\
&\quad\times\cos(\omega_i y)\cos(\omega_{i-k}y)\cos(\omega_{k-p}y)\cos(\omega_p y)\,\mathrm{d}x\,\mathrm{d}y,
\end{aligned}
$$

$$
\begin{aligned}
\bar{K} &= \int_{-1}^{1}\int_{-1}^{1}\cos(\rho_j x)\cos(\rho_{j-l}x)\cos(\rho_{l-q}x)\cos(\rho_q x)\\
&\quad\times\cos(\omega_i y)\cos(\omega_{i-k}y)\sin(\omega_{k-p}y)\sin(\omega_p y)\,\mathrm{d}x\,\mathrm{d}y,\\
\bar{L} &= \int_{-1}^{1}\int_{-1}^{1}\cos(\rho_j x)\cos(\rho_{j-l}x)\cos(\rho_{l-q}x)\cos(\rho_{q-s}x)\cos(\rho_s x)\\
&\quad\times\cos(\omega_i y)\cos(\omega_{i-k}y)\cos(\omega_{k-p}y)\cos(\omega_{p-r}y)\cos(\omega_r y)\,\mathrm{d}x\,\mathrm{d}y,
\end{aligned}
$$

$$
\begin{aligned}
\bar{M} &= \int_{-1}^{1}\int_{-1}^{1}\cos(\rho_j x)\cos(\rho_{j-l}x)\cos(\rho_{l-q}x)\sin(\rho_{q-s}x)\sin(\rho_s x)\\
&\quad\times\cos(\omega_i y)\cos(\omega_{i-k}y)\cos(\omega_{k-p}y)\cos(\omega_{p-r}y)\cos(\omega_r y)\,\mathrm{d}x\,\mathrm{d}y,\\
\bar{N} &= \int_{-1}^{1}\int_{-1}^{1}\cos(\rho_j x)\cos(\rho_{j-l}x)\cos(\rho_{l-q}x)\cos(\rho_{q-s}x)\cos(\rho_s x)\\
&\quad\times\cos(\omega_i y)\cos(\omega_{i-k}y)\cos(\omega_{k-p}y)\sin(\omega_{p-r}y)\sin(\omega_r y)\,\mathrm{d}x\,\mathrm{d}y.
\end{aligned}
$$

Appendix B

The element $[S]_{2M\times 2N}$, $[U]_{2N\times 1}$, and $[V]_{2M\times 1}$ in eqn (33) are:

$$V_m = 0,$$

$$V_{M+m} = \sum_j \sum_i (-1)^j \frac{\rho_j \omega_i}{\rho_j^2 + \omega_i^2} A_{ij}(\tau)\sin(\omega_i y_m) - \sum_j \rho_j (-1)^j [\rho_j E_j \sinh(w_i y_m)$$

$$+\rho_j H_j y_m \cosh(\rho_j y_m) + H_j \sinh(\rho_j y_m)],$$

$$U_n = \mathrm{Re}\, K_n,$$

$$U_{N+n} = \mathrm{Im}\, K_n,$$

$$S_{m,n} = \mathrm{Re}\frac{\partial^2 f_n}{\partial y^2}(1, y_m),$$

$$S_{m,N+n} = -\mathrm{Im}\frac{\partial^2 f_n}{\partial y^2}(1, y_m),$$

$$S_{M+m,n} = \mathrm{Re}\frac{\partial^2 f_n}{\partial x\,\partial y}(-1, y_m),$$

$$S_{M+m,N+n} = -\mathrm{Im}\frac{\partial^2 f_n}{\partial x\,\partial y}(-1, y_m),$$

where Re and Im denote the real and imaginary part of a complex number, respectively, and m, n are integers, $1 \leqslant n \leqslant N$, $1 \leqslant m \leqslant M$.

References

Bardsley, W. (1990) *Progress in Semiconductors*, Vol. 4, p. 155, ed. A. F. Gibson. Wiley, New York.

Chu, J. L. and Lee, S. (1990) Diffusion-induced stresses in two-phase elastic media. *Int. J. Engng Sci.* **28,** 1085–1109.

Chu, J. L. and Lee, S. (1993) Diffusion-induced stresses in a long bar of square cross section. *J. Appl. Phys.* **73,** 3211–3219.

Chu, J. L. and Lee, S. (1994) The effect of chemical stresses on diffusion. *J. Appl. Phys.* **75,** 2823–2829.

Gerald, C. F. and Wheatley, P. O. (1994) *Applied Numerical Analysis*, 5th edn, pp. 268–269. Addison-Wesley, New York.

Hertzberg, R. W. (1983) *Deformation and Fracture Mechanics of Engineering Materials*, 2nd edn, Chap. 11. Wiley, New York.

Hu, S. M. and Schmidt, S. (1968) Interactions in sequential diffusion processes in semiconductors. *J. Appl. Phys.* **39,** 4272–4283.

Hwang, C. C., Wu, C. S. and Hsieh, J. Y. (1993) The effect of curved interface shape on thermal stress during Czochralski. *J. Cryst. Growth* **132,** 523–532.

Hwang, C. C., Chen, K. M. and Hsieh, J. Y. (1994) Diffusion-induced stresses in a long bar under an electric field. *J. Phys. D*: *Appl. Phys.* **27,** 2155–2162.

Iwaki, T. and Kobayashi, N. (1981) Residual Stresses of Czochralski-grown crystal. *ASME J. Appl. Mech.* **48,** 866–870.

Iwaki, T. and Kobayashi, N. (1986) Thermal and residual stresses of Czochralski-grown semiconducting material. *Int. J. Solid Structures* **22,** 307–314.

Kath, W. L. and Cohen, D. S. (1982) Waiting-time behavior in a nonlinear diffusion equation. *Studies Appl. Math.* **67,** 79–105.

King, J. R. (1988) Approximate solutions to a nonlinear diffusion equation. *J. Eng. Math.* **22,** 53–72.

Larché, F. C. and Cahn, J. W. (1982) The effect of self-stress on diffusion in solids. *Acta Metall.* **30,** 1835–1845.

Larché, F. C. and Cahn, J. W. (1985) The interactions of composition and stress in crystalline solids. *Acta Metall.* **33,** 331–357.

Lee, S. and Li, J. C. M. (1981) Dislocation-free diffusion processes. *J. Appl. Phys.* **52,** 1336–1346.

Lee, S. and Ouyang, H. (1987) General solution of diffusion-induced stresses. *J. Thermal Stresses* **10,** 269–282.

Li, J. C. M. (1978) Physical chemistry of some microstructural phenomena. *Metall. Trans.* **9A,** 1353–1380.

Lin, S. and Hwang, C. C. (1995) Nonlinear effect of self-induced electric field on diffusion-induced stresses. *J. Appl. Phys.* **78,** 7035–7039.

Menon, E. S. K., Huang, P., Kraitchman, M., Hoyt, J. J., Chow, P. and de Fontaine, D. (1993) Nonlinear diffusion in Cu–Au multilayer thin films. *J. Appl. Phys.* **73,** 142–149.

Nowinski, J. L. (1978) *Theory of Thermoelasticity with Applications*, Chap. 10. Sijthoff & Noordhoff International Publishers, Alphen Aan Den Rijn.

Prussin, S. (1961) Generation and distribution of dislocations by solute diffusion. *J. Appl. Phys.* **32,** 1876–1881.

Reed-Hill, R. E. (1973) *Physical Metallurgy Principle*, Chap. 18. 2nd edn. Van Nostrand, New York.

Schwendeman, D. W. (1990) Nonlinear diffusion of impurities in semiconductors. *J. Appl. Phys. Math.* **41,** 607–627.

Tuck, B. (1974) *Introduction to Diffusion in Semiconductors*. Peter Peregrinus, London.

Warner, D. D. and Wilson, C. L. (1980) Two-dimensional concentration dependent diffusion. *Bell Sys. Tech. J.* **59,** 1–41.

Weisberg, L. R. and Blanc, J. (1963) Diffusion with interstitial-substitutional equilibrium Zinc in GaAs. *Phys. Rev.* **131,** 1548–1552.